Food Biophysics (2015) 10:195–206
DOI 10.1007/s11483-014-9386-8

ORIGINAL ARTICLE

# Soy β-Conglycinin−Curcumin Nanocomplexes for Enrichment of Clear Beverages

**Shlomit David · Yedidya Zagury · Yoav D. Livney**

Received: 19 February 2014 / Accepted: 2 December 2014 / Published online: 14 December 2014


**Abstract** Delivery of sensitive health-promoting compounds in foods and beverages is an important and timely challenge. Curcumin, a natural polyphenol and the major pigment of the turmeric root, is a potent antioxidant with numerous attributed health benefits. However the major hurdle for applicability of curcumin as a food ingredient is its extremely low solubility in aqueous solutions at both acidic and neutral pH, and its consequent poor bioavailability. Here we have studied the possibility of using the soybean protein β-conglycinin (β-Cg) to form co-assembled nanovehicles for delivery of curcumin in clear beverages, where dietary and religious constraints preclude the use of milk proteins. Using visible light spectrophotometry we found high affinity between β-Cg and curcumin with a binding constant of about $1.27 \cdot 10^6\ M^{-1}$. The curcumin−β-Cg co-assemblies were much smaller than the curcumin aggregates without β-Cg. While in the absence of β-Cg, curcumin aggregates were several microns large and visible by eye, in the presence of β-Cg, particles were much smaller and showed a bimodal size distribution, with modal-average diameters of 27 nm (~90 % of the particles on a volume basis) and 110 nm (~10 %), and average of 46 nm, as measured by dynamic light scattering, and supported by cryoTEM images. Therefore, transparency was maintained in the β-Cg-curcumin co-assembly systems, enabling application in clear beverages. The curcumin – β-Cg system was characterized at increasing molar ratios. The binding sites saturation point of β-Cg was found to be around 15:1 curcumin:β-Cg molar ratio, or about 3 g curcumin/100 g β-Cg. Based on light microscopy observations, the presence of β-Cg both suppressed curcumin crystallization and modified crystal morphology. Moreover, β-Cg−curcumin co-assemblies were found to confer considerable protection to curcumin against light and oxidation induced degradation.

**Keywords** Curcumin · Soy protein · β-conglycinin · Beverages · Nutraceutical delivery

Shlomit David and Yedidya Zagury are equally contributing authors.

**Electronic supplementary material** The online version of this article (doi:10.1007/s11483-014-9386-8) contains supplementary material, which is available to authorized users.

S. David · Y. Zagury · Y. D. Livney (✉)
Biotechnology & Food Engineering, and Russell Berrie nanotechnology Institute, Technion, Israel Institute of Technology, Haifa 3200000, Israel
e-mail: livney@technion.ac.il

## Introduction

Curcumin (bis-α, β-unsaturated β-diketone [1]), is a natural polyphenol found as a major pigment of the root of turmeric (*Curcuma longa* Linn) [1–4], one of three main compounds extracted from the root, called curcuminoids (curcumin, demethoxycurcumin and bisdemethoxycurcumin). Curcumin has a molecular weight of 368.37 Da and a melting point of 183 °C [1]. Curcumin is primarily used as a spice and/or a food coloring agent due to its strong yellow color [1, 3]. It shows remarkable pharmacological activity, including anti-inflammatory [5, 6], anti-proliferative [5], anti-angiogenic [1, 4], antioxidant [1, 4, 6] and wound healing activity [3]. Moreover, many preclinical and clinical trials suggest that curcumin can suppress tumor initiation, promotion and metastasis [5]. The most important properties of curcumin which are responsible for the activities detailed above are its ability to scavenge reactive oxygen and nitrogen free radicals [1, 2, 6–8]. The antioxidant effect of curcumin was found to be eight times more powerful than that of vitamin E [9]. This was attributed to the fact that curcumin consists of two phenolic groups and a β-diketone moiety, all conjugated [3, 8]. Kunchandy and Rao investigated the ability of curcumin to scavenge reactive oxygen radicals at pH 7.4 [6]. They found

that curcumin has a dual action: at higher concentrations it scavenges hydroxyl radicals, whereas at lower ones it activates the Fenton reaction, resulting in increased hydroxyl radical generation. It was also found that the curcumin is a potent scavenger of superoxide radicals. This property may be responsible for the anti-inflammatory activity of curcumin [6]. Other studies [1] showed similar results, − i.e. that curcumin may possess pro-oxidant or antioxidant activity, depending on dose and chemical environment (e.g. $Cu^{2+}$ ions).

Pharmacologically, curcumin was found to be safe [5], however the major problem of curcumin applicability as a health promoting agent, and particularly as a food ingredient, is its extremely low solubility in aqueous solutions, both at acidic and neutral pH, and hence, its poor bioavailability [7]. In aqueous solutions curcumin is exposed to hydrolytic degradation reactions which are accelerated at pH above neutral [7]. The main decomposition products have been identified as feruloyl methane, ferulic acid and vanillin [7, 10]. Vanillin is a secondary degradation product formed by hydrolysis of feruloyl methane [7]. According to Tønnesen et al. an accurate measurements of the degradation rate is difficult to obtain at neutral and lower pH due to the low solubility of curcumin [7]. Curcumin is sensitive to light but is moderately stable to heat [11]. Curcumin was found to decompose under exposure to light in organic solvents [7].

So far, two approaches have been adopted to improve the water dispersibility of curcumin. The first method was to synthesize a curcumin derivative that has a polar substituent [3]. In the second method curcumin is incorporated into different water soluble hosts like β-Lactoglobulin [12] or cyclodextrins [3, 7]. Apparently, curcumin binds to water soluble hosts by a combination of the hydrophobic effect, van der Waals interactions and hydrogen bonds.

Dispersing curcumin by complexation with various macromolecules (like gelatin or polysaccharides) has been attempted (mainly for coloring applications), however, it was done under alkaline conditions, where curcumin decomposes within minutes [7]. Hence, complex formation under low, or neutral pH, as performed in the current study, are preferable approaches and are more suitable for food applications. Tønnesen et al. reported that in some cases, complex formation of curcumin and cyclodextrin had a destabilizing, rather than a stabilizing effect on the photodegradation process of curcumin [7].

Previous studies from our lab evaluated milk proteins [13] like casein micelles [14–16], casein-maltodextrin Maillard conjugates [17], and whey proteins (like β-Lactoglobulin [18, 19] and its complexes with pectin [20, 21]), as nanovehicles for nutraceuticals, particularly hydrophobic, poorly water soluble ones, in food and beverage applications. However, in some cases, the use of milk proteins is ruled out due to religious (Kosher Parve) or dietary (vegetarian, vegan) constraints. Hence, we wished to evaluate the use of an inexpensive widely available plant protein, such as soybean protein, for nanodelivery of an important hydrophobic nutraceutical such as curcumin.

Soybean Protein Isolate (SPI) is a powder rich in proteins made from defatted soybeans. SPI is in widespread use in food manufacturing due to its good functional properties, low cost, wide availability and high nutritional value. Soybean proteins have excellent gelation capability and good emulsifying and emulsion stabilizing abilities [22, 23]. Nearly 90 % of the soybean proteins are storage proteins, mostly consisting of glycinin (the 11 s fraction, ~52 % of the protein) and β-Cg (the 7 s fraction, ~35 % of the protein) [24, 25]. Both glycinin and β-Cg have quaternary structures.

B-Cg is a glycoprotein with a molecular mass of 150–200 kDa and is a trimer whose three subunit types are α (68 kDa), α′ (72 kDa) and β (52 kDa) [22]. These subunits increase in emulsifying properties: $\alpha > \alpha' >> \beta$ [25]. Seven isoforms, containing various combinations of these subunits, are observed in nature [24, 26]. While the β subunit does not have any cysteine residue (characterized by the –SH functional group), the α and α′ each has one cysteine residue near its N-terminus. None of the subunits has any cystine (-SS-) residue [22]. Moreover, while the α and α' subunits are each composed of a core region, which is more hydrophobic, and a more hydrophilic extension region, the β subunit consists only of the core region [27]. The trimer is held together by hydrophobic interactions between the subunits' core regions [28]. The isoelectric point of β-Cg is pH 4.8−4.9 [27] and those of the isolated subunits are α: 4.9, α′: 5.18 and β: 5.66-6 [29].

Grace et al. and Roopchand et al. found that soy proteins could stably bind and concentrate cranberry polyphenols to form a cranberry polyphenol–SPI complex. They showed that complexation with SPI stabilized and preserved the integrity of the polyphenols for at least 15 weeks at 37 °C [30, 31]. Another use of soy protein as a carrier for bioactives was demonstrated by Wan group [32]. They investigated the potential of SPI as an emulsifier to improve the effectiveness of resveratrol (RES) as a natural antioxidant in corn oil-in-water emulsions. Tapal and Tiku recently investigated the potential of SPI as a carrier for curcumin [33]. They suggested that the curcumin molecules interact with soy proteins by binding to the low polarity regions of the proteins. Furthermore, they found that the effective water dispersibility of curcumin was increased thanks to the complexation. However, the potential of β-Cg alone as curcumin carrier has not yet been investigated. The emulsifying and emulsion-stabilizing abilities of β-Cg are much stronger than those of glycinin [22, 25] hence it shows better promise than glycinin or whole SPI as a natural nanocarrier for lipophilic bioactives in aqueous systems. We have recently explored the potential of β-Cg as a carried for vitamin D [34]. The objective of the current work was to explore the potential of β-Cg as a nanovehicle for curcumin,

and to evaluate its performance in terms of dispersion and protection capabilities, for the application in food and beverage applications, particularly where milk proteins cannot be used, e.g. in products for vegan consumers, or for Kosher-Parve products. As β-Cg shows good solubility 1–2 pH units above (or below) its pI, we expected it to be suitable for the dispersion of hydrophobic nutraceuticals even in clear beverages of around neutral (and low) pH. We focused on neutral pH values, typical for a major beverage category, mineral water (6.7-7.3) and for water enriched with vitamins and nutraceuticals.

## Materials and Methods

### Materials

Curcumin (CAS registry number 458-37-7) (purity >95.0 % by TLC) was purchased from Sigma Aldrich (Rehovot, Israel). β-Cg fraction (BCF) was kindly donated by Solbar Ltd. (Ashdod, Israel, CHS Inc. Minnesota, USA).

### Methods

#### *Solution Preparation*

To promote self-assembly of the β-Cg (and co-assembly with curcumin) we used 30 mM phosphate buffer which, according to the literature [35], suppresses the dissociation to monomers observed at very low ionic strength around neutral pH, and favors the protomer (trimer) and even dimer (hexamer) quaternary structures of the pure protein. A 30 mM phosphate buffer solution (target: pH 7) containing 0.02 % sodium azide (as experimental preservative, not for food use!) was prepared as follows: 0.234 g $NaH_2PO_4 \cdot 2H_2O$, 0.267 g $Na_2HPO_4 \cdot 2H_2O$ and 0.02 g sodium azide ($NaN_3$) were dissolved in 100 ml HPLC grade water. The buffer was used without further pH correction. The exact final pH of the solution was 6.8. The β-Cg solution was prepared from the BCF powder received from Solbar, as follows: 200 mg of powder were dissolved in 40 ml phosphate buffer (30 mM, pH 6.8) and shaken mechanically at room temperature overnight. The next day, the solution was centrifuged at 15,000 g for 15 min and filtered through a 0.45 μm filter by vacuum, to remove any undissolved matter. The remaining protein concentration was quantified by the Bradford assay using a Sigma Bradford reagent and a BSA standard diluted to 5.26 μM (1 mg/ml) stock. The molar β-Cg concentration was calculated assuming that the molecular mass of β-Cg is 190 KDa [29, 36].

To incorporate the curcumin in the protein nanoparticles we employed a method we used in previous studies in our group [14–16], which is a modified antisolvent approach. Liquid antisolvent processes are based on the use of two liquid solvents that are completely miscible, one being a good solvent for the active compound, and the other a poor solvent. Usually the addition of the antisolvent induces the supersaturation and precipitation of the active compound [37]. In the currently used method, however, the goal is to form soluble nanocapsules wherein curcumin is entrapped within β-Cg. Also, as opposed to most antisolvent approaches where the final volume percent of the good solvent (e.g. ethanol) after mixing is high, in the current method the percent of added ethanol is very low (typically ≤2 %), and may become negligible after an additional dilution in the final beverage, and certainly after freeze drying and reconstitution in water.

Curcumin stock solution was prepared at the desired concentration in pure ethanol. These stocks were added dropwise to phosphate buffer or to β-Cg solution while vortexing, bringing the sample to a final ethanol concentration of 2 %. The samples were shaken mechanically at 4 °C overnight for equilibrium to be reached. The addition of β-Cg or curcumin did not modify the pH of the solution.

#### *Characterization of the β-Cg – Curcumin Complexes*

For the initial characterization, an ethanolic solution of 336 μM curcumin was added dropwise to phosphate buffer (30 mM) both with and without 5.26 μM (1 mg/ml) β-Cg, while vigorously stirring. The samples were filtered at 0.45 μm and a photo of the filtered and unfiltered samples was taken. Because those concentrations were too high for spectrophotometer measurement, solutions of a same molar ratio were prepared at a concentration 10 times lower and then measured by a spectrophotometer. The absorbance spectra were measured for the samples before and after filtration to ascertain the presence of curcumin in the filtrate. The samples were filtered to qualitatively show that in the presence of the protein the typical particle diameter decreased below 0.45 μm. The blank solution was 3 mM phosphate buffer pH 6.8, with 2 % ethanol. All spectroscopic measurements in this study were performed using an Ultrospec 3000 spectrophotometer (GE Healthcare, Waukesha, Wisconsin, USA), using a 1 cm path length cuvette.

For the characterization of the curcumin−β-Cg complexes at different molar ratios, solutions of 5.26 μM (1 mg/ml) β-Cg in 30 mM phosphate buffer with increasing curcumin concentrations were prepared. The molar ratios examined were 0:1, 3:1, 6:1, 9:1, 12:1, 15:1, 20:1, 35:1, 45:1, 50:1 and 55:1 curcumin:β-Cg. The samples were stored at 4 °C for 2 weeks, and then the absorbance of the upper clear liquid was measured at 330 nm. Although the maximal absorbance of curcumin is at 424 nm, because the absorbance at 424 nm was too high at the higher curcumin concentrations (above 35:1 Molar ratio), the absorbance at 330 nm was chosen for the examination in the entire experiment. Before

the spectrophotometry measurement the samples were not vortexed in order to prevent the curcumin sediment from mixing with the upper liquid.

*Binding Constant Determination*

The binding constant was determined using two methods: the Benesi-Hildebrand method [2, 38] and the reciprocal plot [2, 39], using the absorbance at 424 nm of curcumin in phosphate buffer and varying the final concentration of β-Cg. The final curcumin concentration was 15 μM. As a control, a 5.26 μM (1 mg/ml) β-Cg solution with 2 % ethanol was prepared. A solution of phosphate buffer (30 mM, pH 6.8) with 2 % ethanol was used as a blank. The extinction coefficient of β-Cg, $\varepsilon_{\beta\text{-Cg}}$, at 424 nm was determined according to Beer-Lambert law [40], as described in the supplementary information.

*Particle Size Distribution Analysis by Dynamic Light Scattering (DLS)*

DLS was used to evaluate size distribution of the β-Cg curcumin nanocomplexes at different molar ratios, and that of the pure protein. Solutions containing 5.26 μM (1 mg/ml) β-Cg in phosphate buffer (30 mM, pH 6.8) with and without curcumin at increasing final concentration (in the range of 0:1–15:1 curcumin:β-Cg molar ratios) were measured. The measurements were carried out using a DLS analyzer (NICOMP$^{TM}$ 380 Particle Sizing Systems Inc., Santa Barbara, CA, USA) equipped with an Avalanche photo diode (APD) detector, at a fixed angle of 90°. The 90 mW laser wavelength was 658 nm. Mono- and bi modal distributions were calculated from the scattered light intensity fluctuations, by cumulants NICOMP$^{TM}$ analysis of the auto correlation function (observed size range: 1–1000 nm). The examinations were done using round cuvettes.

*Light Microscopy Imaging*

Light microscopy images of 5.26 μM β-Cg in phosphate buffer (30 mM, pH 6.8) and of 15, 30 and 100 μM curcumin in phosphate buffer were compared to images of the same curcumin concentrations complexed with β-Cg (3:1, 6:1 and 20:1 curcumin:β-Cg molar ratio). The samples were shaken mechanically at 4 °C overnight before analysis. Light microscopy images were taken at×60 magnification using an Olympus BX51 light microscope, operated in bright-field or polarized light optical mode.

*Cryogenic Transmission Electron Microscopy (Cryo-TEM) Imaging*

For Cryo-TEM imaging, samples of 5.26 μM β-CG solutions, pH 6.8, were prepared both alone and with curcumin added, as described above, with a final curcumin concentration of 15 μM and 30 μM (molar ratio of 3:1 and 6:1 respectively). The specimens were prepared as thin liquid films (10–500 nm thick), on perforated polymer/carbon films in a controlled-environment vitrification system at 25±0.01 °C and 95–99 % relative humidity, and then quench-frozen in liquid ethane at its freezing point (−183 °C). This process is designed to prevent water crystallization during thermal fixation. In this manner, component segregation and rearrangement are mostly prevented, and the original fluid nanostructure is preserved. Images were recorded at a 120 kV acceleration voltage, in a low-dose mode, to minimize electron-beam radiation damage. Gatan Multi Scan 791 cooled CCD camera was used to acquire the images, with the Digital Micrograph 3.1 software package.

*Evaluation of the Protection of Curcumin by β-Cg Against Light and Oxygen Using Spectrophotometry: "Accelerated Shelf Life" Test*

To evaluate the protection of curcumin by β-Cg against both light and oxygen, samples were exposed to stress test conditions. Curcumin was dissolved in ethanol, and then added to a phosphate buffer (30 mM, pH 6.8) with 5.26 μM (1 mg/ml) β-Cg, to a final curcumin concentration of 15 μM. The final volume of each solution was 4 ml. Controls of curcumin without β-Cg and of β-Cg without curcumin were prepared as well. After preparation, the vials were covered with aluminum foil and shaken mechanically at 4 °C overnight to reach equilibrium. Then, the aluminum foil was removed to expose the solutions to light and the tube lids were replaced with parafilm, exposing the solutions to oxygen (Parafilm $O_2$ permeability at 23 °C is~350 $cm^3/m^2$ in 24 h [41]). The vials were shaken at room temperature. Absorbance at 424 nm was examined at 0, 1, 4, 24, 46, 93 h and a week after the solutions preparation. A solution of phosphate buffer (30 mM, pH 6.8) with 2 % ethanol served as the blank. Measurements were made in triplicate. The accelerated shelf life test was analyzed using OriginLab software (version 8).

## Results and Discussion

Spectroscopic Characterization of the β-Cg – Curcumin Complexes

To characterize the β-Cg−curcumin system, solutions of 336 μM curcumin in phosphate buffer, were prepared both with and without 5.26 μM (1 mg/ml) β-Cg, in each case, before and after filtration through a 0.45 μm filter. The samples were filtered in order to show that in the presence of the protein the particle diameter decreased below 0.45 μm, rather than to remove unwanted elements in the solution. The inset in

Fig. 1 displays a photo taken 24 h after preparation. Due to the high absorbance of the samples shown in the inset, solutions of same ratio have been prepared at a concentration 10 times lower for the absorbance spectra measurement. The absorbance spectra are displayed in Fig. 1.

Curcumin is a very hydrophobic molecule (log P is 2.23–2.30 [42]) that has very poor solubility in aqueous solutions [7]. Consequently, large aggregates formed in the phosphate buffer not containing β-Cg (Fig. 1, vial 2: Notice the aggregates at the air-water surface and on the bottom of the vial). The aggregates at the surface apparently accumulated there (despite their higher density compared to that of the solution) due to low wettability of this hydrophobic material. Filtration of this dispersion using a 0.45 μm filter, removed all visible curcumin aggregates (Fig. 1 vial 1). In contrast, in the solution containing β-Cg (as can be seen in Fig. 1 vial 3), no aggregates could be seen by eye and the system looked homogeneous. Filtration using a 0.45 μm filter, removed only some of the dispersed curcumin (Fig. 1 vial 4, compared to vial 3). This shows that in the presence of β-Cg smaller particles of curcumin were obtained, most of which passed the 0.45 μm filter. These qualitative results were complemented quantitatively by recording the absorbance spectra of the different systems following their 10 fold dilution; before filtration the solutions with and without β-Cg had a peak typical of curcumin (maximum around 424 nm [2, 3]). According to the lack of visible curcumin in vial 1 and the very low absorbance of the corresponding solution, it can be concluded that in the absence of β-Cg, after filtration at 0.45 μm practically no curcumin passed the filter. This indicates that essentially all curcumin aggregates before filtration (vial 2) were larger than 0.45 μm. On the other hand, the filtrate of the β-Cg - curcumin solution was yellowish, and its absorbance spectrum showed that curcumin was present in the system. These also indicated that nanocomplexes, smaller than 0.45 μm, had been obtained in the presence of β-Cg. Although the protein decreased the particle size, the system was not colloidally stable over time, and a week later sediment was observed. Therefore it can be concluded that at this molar ratio the β-Cg was above its binding sites saturation point.

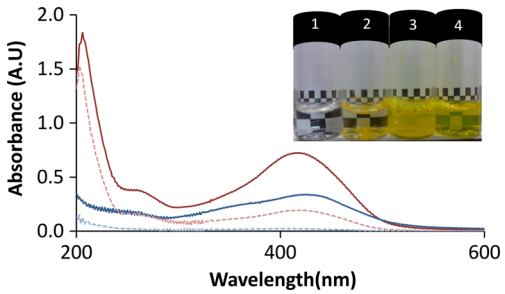


**Fig. 1** The absorbance spectra of β-Cg complexed with curcumin and curcumin alone before and after filtration at 0.45 μm. β-Cg concentration was 0.526 μM (0.1 mg/ml) in 3 mM phosphate buffer and curcumin final concentration was 33.66 μM (molar ratio of 66:1 Curcumin:β-Cg). Solid lines and dashed lines represent the absorbance before and after filtration (0.45 μm) respectively, blue (lower solid/dashed line) is curcumin alone, and red is curcumin with β-Cg. Inset: vials (1,2) contained 336 μM curcumin in 30 mM phosphate buffer after and before filtration at 0.45 μm, respectively; vials (3,4) contained 336 μM curcumin and 5.26 μM (1 mg/ml) β-Cg in 30 mM phosphate buffer (molar ratio of 66:1 Curcumin:β-Cg) before and after filtration at 0.45 μm, respectively. The samples shown in the inset are at same molar ratio, but at 10 fold higher concentrations, compared to those used for the absorbance measurement

The curcumin – β-Cg system was then characterized at different molar ratios to estimate the binding sites saturation point and loading capacity of β-Cg, and to observe the effect of the ratio on colloidal stability. Solutions of different curcumin:β-Cg molar ratios (0:1–55:1) containing 5.26 μM β-Cg and increasing curcumin concentrations in the range of 0 to 275 μM were prepared, and after 2 weeks at 4 °C some sedimentation was observed at the high curcumin concentrations. The absorbance of the upper clear liquid was measured at 330 nm, as displayed in Fig. 2. It is interesting to see that while the absorbance increased with increasing curcumin concentration at a constant protein concentration, there were two ranges in the graph, suggesting of two consecutive processes which occur: up to about 15:1 molar ratio (75 μM curcumin), there was apparently a rising absorbance which tended towards a horizontal saturation asymptote (absorbance of about 0.7), but then, there was a new rise in absorbance, which again seems to tend toward a higher plateau (absorbance of about 1.5) above 50:1 (250 μM curcumin). At the higher range above 20:1 molar ratio, yellow sediment was also observable by eye after calm equilibration. We suggest that at molar ratios below 15:1 the curcumin was well entrapped and dispersed by the β-Cg, and this saturation of the protein loading produced the first "Langmuir-type" saturation curve. However, at molar ratios of 20:1 and above, the protein was apparently above its maximal loading capacity, and the unbound curcumin aggregated into large particles and precipitated, hence, another rise in absorbance was observed, and sediment appeared after settling. The binding affinity and the maximal loading were further studied as described below.

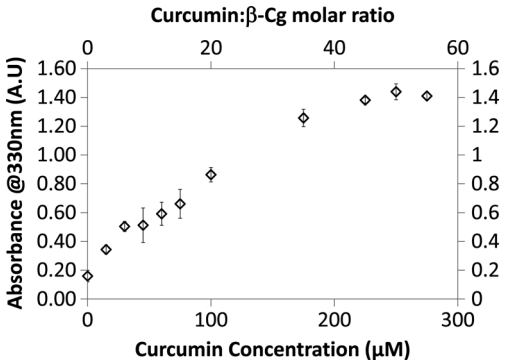


**Fig. 2** The absorbance at 330 nm of solutions with different curcumin:β-Cg molar ratios and increasing curcumin concentrations in the range of 0 to 275 μM. All solutions contained 5.26 μM β-Cg in a 30 mM, pH 6.8 phosphate buffer

Binding Studies by Absorbance Spectra Measurement

The binding constant of curcumin to β-Cg was determined using mathematical analysis of the absorbance spectra of phosphate buffer solutions containing a constant concentration of curcumin (15 μM) and rising concentrations of β-Cg (0.0526–5.26 μM) (Fig. 3).

Two methods were used for the binding constant determination: the Benesi- Hildebrand method and the reciprocal plot method. The Benesi-Hildebrand method [2, 38], which is typically applied to reaction equilibria of one-to-one complexes such as host-guest molecular complexation, was used for the determination of the equilibrium constant of the studied non-covalent interactions. At 424 nm, curcumin shows a maximum peak in the absorbance spectrum, while β-Cg shows negligible absorbance (Fig. 3). Moreover, it can be seen that in the presence of increasing concentrations of β-Cg there is an increase in the maximum of the solution absorbance around 424 nm. Likewise, there is a gradual redshift in the peak wavelength with rising β-Cg concentration. Therefore, the absorbance at 424 nm was used to estimate the binding constant [2]. The Benesi Hildebrand equation [2, 43] (Eq. 1) is written in terms of absorbance change at 424 nm as a function of the reciprocal concentration of β-Cg:

$$\frac{1}{\Delta A} = \frac{1}{K \cdot \Delta\varepsilon_{424} \cdot [\text{curcumin}]} \cdot \left(\frac{1}{[\beta\text{-}Cg]}\right) + \frac{1}{\Delta\varepsilon_{424} \cdot [\text{curcumin}]} \quad (1)$$

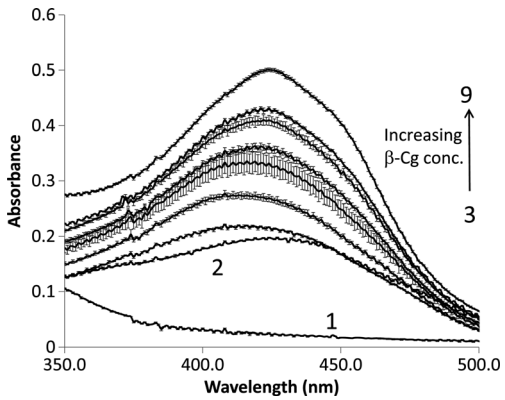


**Fig. 3** Absorbance spectra of phosphate buffer (30 mM, pH 6.8) solutions containing 15 μM curcumin with varying final concentrations of β-Cg from 0.0526 to 5.26 μM (0.01–1 mg/ml). Spectrum 1 corresponds to 5.26 μM β-Cg without any curcumin. Spectrum 2 corresponds to 15 μM curcumin without any β-Cg. Spectra 3–9 correspond to 15 μM curcumin with 0.0526, 0.263, 0.526, 1.05, 1.58, 2.11, 5.26 μM β-Cg. Samples were not filtered after preparation and before absorption spectra measurements

ΔA is the change in absorbance at 424 nm at different concentrations of β-Cg varying from 0.0526 to 5.26 μM:

$$\Delta A = A_{[[\beta\text{-Cg}];[\text{curcumin}]=15\mu M]} - A_{[[\beta\text{-Cg}]=0;[\text{curcumin}]=15\mu M]} \quad (1a)$$

[β-Cg] and [curcumin] are the molar concentrations of these compounds. $\Delta\varepsilon_{424}$ is the differential extinction coefficient at 424 nm. According to a double reciprocal linear plot of the Benesi Hildebrand equation (Fig. 4), by dividing the intercept by the slope, a binding constant of $(0.82\pm0.04)\cdot 10^6\ M^{-1}$ was obtained.

The reciprocal plot method [39] (Eq. (2)) is another method, which allows calculating both the affinity constant of a ligand with a protein and the number of binding sites. The experimental analysis method we used is based on Barik et al. [2], except we kept the ligand (curcumin) concentration constant and varied the protein (β-Cg) concentration. This was done, because a spectral region, where only one of the two molecules and also the complex absorb, was only found around 424 nm, where curcumin and the complex absorb, but not the protein, as explained above.

$$\frac{1}{r} = \frac{1}{n \cdot K} \cdot \left(\frac{1}{[\beta\text{-}Cg]}\right) + \frac{1}{n} \quad (2)$$

K is the binding constant of β-Cg and curcumin molecules. Originally, in the reciprocal plot, n is the number of binding sites on a macromolecule, and r is the fraction of binding sites on the macromolecule that are occupied by the ligand. However, here, due to the fact we kept the curcumin concentration constant and raised the protein concentration following the rise in the absorption of the complex, we defined r as the fraction of the curcumin molecules in the system which are bound to the protein, and n as the "number of β-Cg molecules bound per molecule of curcumin in the complex upon binding saturation" (i.e. 1/n is the number of binding sites for curcumin in a molecule of β-Cg). Here too, the change in

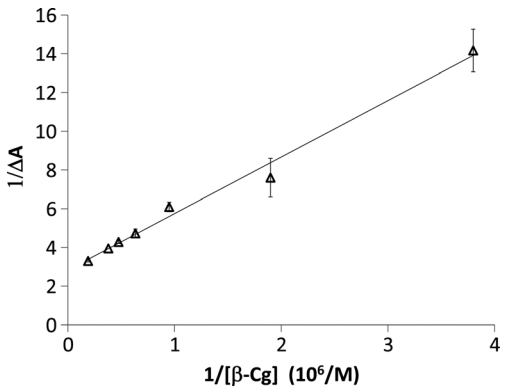


**Fig. 4** The double reciprocal linear plot according to the Benesi-Hildebrand equation. Linear fit result: $y=2.92\times+2.83$; $R^2=0.99$

absorbance at 424 nm ($\Delta A_{424}$) was used to estimate r (Eq. (3)):

$$r = \frac{\Delta A_{424}}{[\text{curcumin}] \cdot l \cdot \varepsilon_{[424\text{curcumin},\beta\text{-Cg complex}]}} \quad (3)$$

where l is the optical path length which equals 1 cm. The curcumin molar concentration was 15 μM. $\varepsilon_{424[\text{curcumin, β-Cg complex}]}$, the extinction coefficient of the curcumin β-Cg complex at 424 nm, was found to be 39,003 $M^{-1}$ $cm^{-1}$, as described in the supplementary information.

From the plot of 1/r vs. 1/[β-Cg] (Fig. 5), a binding constant of $(1.72\pm0.09)\cdot10^6$ $M^{-1}$ was obtained, which evidences a high affinity binding. When comparing the binding constant values obtained by the two methods it can be seen that both yielded binding constants of around $10^6$ $M^{-1}$. Interestingly, according to the literature [3], the binding constant of curcumin with different surfactant micelles (both neutral and charged surfactants) ranged between $10^4$ and $10^5$ $M^{-1}$, hence, the binding constant found for β-Cg and curcumin indicates a much more significant affinity with this protein compared to that with low molecular weight surfactants.

The number of binding sites (1/n, eq. 2) available for curcumin in β-Cg was found to be 1.065, which means that the molar binding ratio of curcumin:β-Cg is about 1:1. This further confirms the validity of using the Benesi Hildebrand equation, which assumes a 1:1 binding ratio [2]. However, the fact that the molar ratio at saturation based on the absorbance results (Fig. 2) was much higher, i.e. around 15:1 curcumin:β-Cg, suggests that while on a molecular level there is a 1:1 binding, in effect, small nanoaggregates (or nanocrystals) are most probably formed and entrapped within the protein nanoparticles so that most of the entrapped curcumin molecules are not directly bound to the protein. To accurately determine the maximal loading of the protein, DLS, light microscopy and cryoTEM microscopy experiments were conducted for increasing molar ratios, as discussed below.

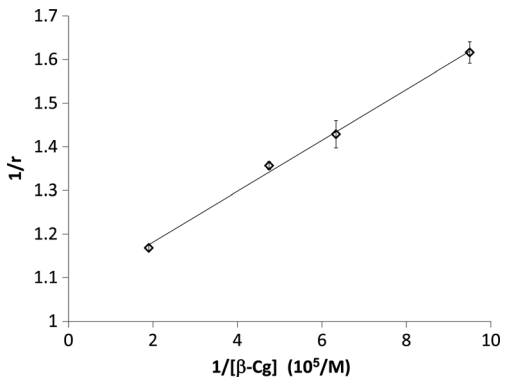


**Fig. 5** The linear plot for 1/r as a function of 1/[β-Cg] according to the reciprocal plot. Linear fit result: y=0.058×+1.065; $R^2$=0.980

## Particle Size Distribution

Figure 6a shows particle size distribution for β-Cg (5.26 μM) and β-Cg−curcumin nanocomplexes (12:1 Molar ratio). In the presence and absence of curcumin, bimodal distributions of particles were formed. For β-Cg, one population observed, with a mean diameter of 27 nm, accounts for ~85 % of total particles volume, and a second population, with a mean diameter of ~110 nm, accounts for the remaining 15 %. It can be seen that in the presence of curcumin a similar bimodal distribution with slightly larger diameters was observed (Fig. 6a). Due to the high binding affinity, and lack of visually observed sediment, it is reasonable to determine that the new peaks represent protein-curcumin complexes. The particle size of curcumin without β-Cg was of a few microns (e.g. Fig. 1, vial 2), hence not measurable by the DLS analyzer (which is only applicable in the range of 1-3000 nm). Analyzing the DLS data, it is possible to deduce that complex formation with β-Cg prevented curcumin aggregates from growing into large micron-sized particles. This is supported by the light microscopy findings (Fig. 7).

To further study the effect of the curcumin:β-Cg ratio on particle size distribution, solutions of different curcumin concentrations were added to a constant β-Cg concentration to create nanocomplexes comprised of curcumin:β-Cg at molar ratios in the range of 0:1 to 15:1. Again, the size distribution of the nanoparticles in the solutions seemed to consist of two sub-populations in all ratios studied. The first sub-population included small particles in the range of 20–70 nm in diameter. The second sub-population included nanoparticles of 70–200 nm. To analyze how increasing curcumin concentrations affected the particle size of the complexes, the volume fraction in each sub-population was plotted against curcumin:β-Cg molar ratio (Fig. 6b). The results show that from 0:1 to 12:1 curcumin:β-Cg molar ratios the volume-weighted percents of the sub-populations remained quite constant. The volume-weighted average particle size of the curcumin- β-Cg complexes from 3:1 to 15:1 was 46±7 nm (the standard deviation here is that of the averages at the different ratios). In comparison, SPI-curcumin nanoparticles reported in the literature were much larger, 220 to 287 nm on average [44], demonstrating an important advantage of β-Cg over SPI, particularly in clear beverage applications. However, for molar ratios above 12:1 (e.g. 15:1), a minor increase in the volume-weighted percent of large particles, and a minor decrease in that of the small particles were observed. We suggest that this is an indication that the loading capacity has been reached, and surplus cucrcumin starts forming larger aggregates. Notably, for molar ratios above 15:1 the DLS analyzer indicated the presence of large (>3000 nm) particles. Therefore, samples of these molar ratios (20:1, 35:1 curcumin:β-Cg) were imaged by light microscopy (see below). The presence of large

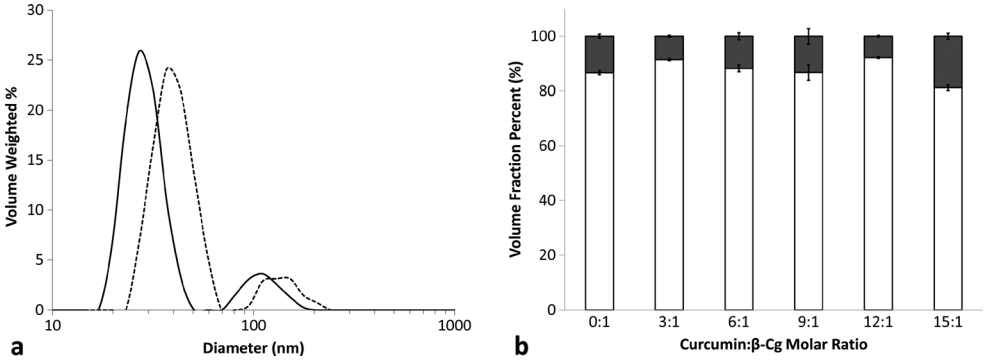


**Fig. 6** **a** Volume-weighted size distributions of β-Cg (solid line) and nanocomplexes of curcumin:β-Cg (12:1 Molar ratio) (dashed line), obtained by DLS. **b** curcumin-β-CG particle size distribution characteristics at varying molar ratios. The bars represent the volume fraction percent of the smaller, 20–70 nm, particles (white) and that of the larger, 70–200 nm particles (gray)

particles (>3000 nm) suggests that the binding sites saturation of β-Cg is around 15:1 molar ratio.

Assuming 15:1 is the maximal molar loading ratio, then 3 g of curcumin may be loaded per 100 g of β-Cg. This is higher than the maximal loading capacity of 2.7 g/100 g reported for SPI [44]. Apparently, at 20:1 Molar ratio and above, i.e. above the β-Cg saturation point, excess curcumin formed large crystalline structures. Clearly, the presence of β-Cg inhibited curcumin crystallization, at least up to the protein saturation point. These conclusions were well supported by the polarized light microscopy results displayed below (Fig. 7).

## Light Microscopy

Figure 7 shows images obtained by bright-field and polarized light microscopy (respectively) of: (a, g) β-Cg alone (5.26 μM); curcumin alone (b, h: 15 μM and d, j: 30 μM) and in the presence of 5.26 μM β-Cg (c, i: 15 μM curcumin, e, k: 30 μM curcumin, and f, l: 100 μM curcumin). It is evident from Fig. 7 that when curcumin, that was dissolved in ethanol and added dropwise to an aqueous (protein free) buffer solution, it formed distinctive and relatively large crystals of ~100 and ~40 μm in diameter, at final curcumin concentrations of 15 and 30 μM respectively (Fig. 7b and d). The fact that curcumin was in a crystalline form was evidenced by the polarized light optical mode [45] (Fig. 7h and j). Such crystals cause turbidity and precipitate, which is unappealing for consumers, and dramatically diminishes the beneficial health effects, due to the significantly reduced bioavailability of crystalline material [46]. In contrast, in the presence of the protein, it can be seen that as long as the molar ratio was below 15:1 (e.g. 3:1 and 6:1, Fig. 7c and e) no aggregates or crystalline structures were observed (Fig. 7i and k), only nanoscale particles were found in these samples, based on the DLS analysis and the cryoTEM imaging (discussed below). However, above a 20:1 molar ratio (100 μM curcumin, Fig. 7f, l) crystallization of the surplus unencapsulated curcumin is observed. Hence, according to the light microscopy and DLS results, below the saturation of the protein binding sites the complexation of the curcumin with β-Cg suppressed curcumin crystallization. We have recently observed a similar effect of another amphiphilic protein, β-casein, on the crystallization of a hydrophobic drug, paclitaxel [47].

During the light microscopy analysis we noticed that as curcumin concentrations in phosphate buffer increased, the crystal size decreased. This may be explained by the well-known phenomenon in crystallization processes: as the

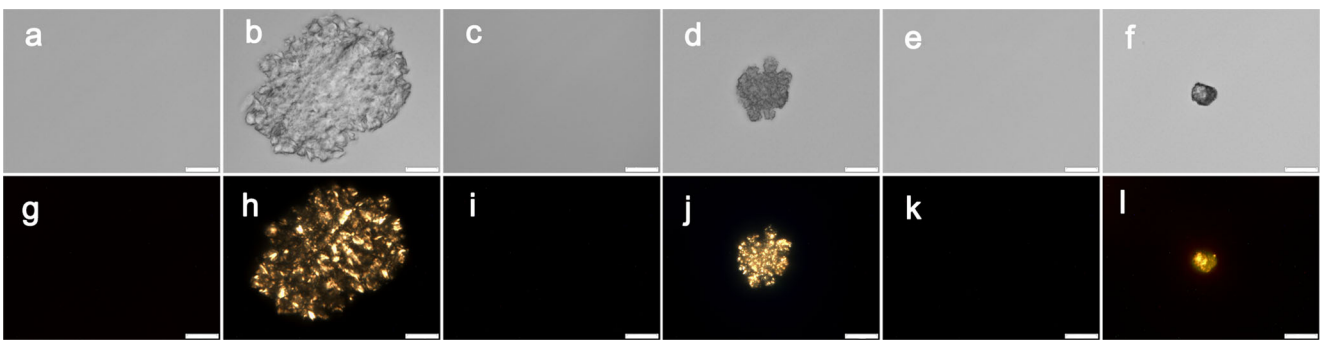


**Fig. 7** Light microscope images of (**a**) β-Cg (5.26 μM) in phosphate buffer, (**b**) and (**d**) 15 μM and 30 μM curcumin in phosphate buffer respectively, (**c**) and (**e**) curcumin:β-Cg 3:1 and 6:1 molar ratio, respectively (at corresponding curcumin concentrations: 15 μM and 30 μM), and (**f**) curcumin:β-Cg 20:1 molar ratio (100 μM curcumin). Images (**a**)–(**f**) are in bright-field optical mode, while (**g**)–(**l**) are the same samples under a polarized light optical mode. Scale bars: 20 μm

supersaturation increases, nucleation rate increases, resulting in more numerous but smaller crystals.

Besides the size difference, it is remarkable to see that there is a difference in the morphology of the curcumin crystals in the presence and absence of β-Cg (Fig. 7b and d compared to 7f). Certain proteins have the ability to adsorb onto the surface of certain crystals, suppress their growth [47] and sometimes modify their morphology (by preferential adsorption to certain crystal-faces), e.g. as was observed with some antifreeze (ice-binding) proteins [48, 49].

## Cryogenic Transmission Electron Microscopy (Cryo-TEM)

Figure 8 shows cryo-TEM images of β-Cg in phosphate buffer, and curcumin:β-Cg at 3:1 and 6:1 molar ratio, respectively. One can see that there are several self-assembled forms of β-Cg in the phosphate buffer: large (~ 100 nm) fairly circular clusters (Fig. 8a, arrow 1) and small protein aggregates, around 10–20 nm diameter (Fig. 8a, arrow 2). The size of the self-assembled forms imaged by Cryo-TEM is consistent with the bimodal results of the DLS. There are two typical sizes of β-Cg nanoparticles: one around 20 nm, and another around 100 nm. It may be that the larger particles are clusters of small ones, and they may result from some heat-treatment history of the soy protein during its production. In solutions of curcumin:β-Cg complexes (Fig. 8b and 8bc), the two typical forms of protein aggregates were seen, but unlike the β-Cg alone, many dark dots were observed entrapped within them. These points most likely indicate the curcumin nanoparticles or nanocrystals co-assembled with the β-Cg. It is important to note that the dark points were seen only within the protein aggregates (small and large), which is in line with the fact it is very poorly soluble, and prefers adhering to the protein, and also supports our hypothesis that curcumin associates with the hydrophobic regions of β-Cg. This is also in line with literature results suggesting curcumin interacts with non-polar regions of SPI [33]. Here, too, the particles sizes were compatible with the DLS results: no significant difference was observed upon addition of curcumin to a final molar ratio of 3:1 or 6:1 compared to 0:1. Comparison of the curcumin:β-Cg solutions with rising curcumin concentrations (Fig. 8b vs. 8c) shows that as the curcumin concentration increased, there were more curcumin nano-crystals (dots) entrapped within the protein nanoparticles. Moreover, the dots are darker in the higher curcumin concentration due to the higher density of the curcumin molecules.

## Protection of Curcumin by β-Cg Against Both Light and Oxygen Induced Degradation During an "Accelerated Shelf Life" Test, Using Visible - Light Spectrophotometry

It has been reported in the literature that soy proteins provide protection to various bioactives by encapsulating them. For instance, Nori et al. found that encapsulation of propolis with soy protein preserved the phenolic and flavonoid compounds present in free propolis [50]. To examine the protection conferred to curcumin by β-Cg against light and oxygen induced degradation, an "accelerated shelf life" study was conducted over 7 days under stress conditions. Solutions containing 15 μM curcumin in phosphate buffer (30 mM, pH 6.8) with 5.26 μM (1 mg/ml) β-Cg were compared to pure curcumin solutions and the absorbance at 424 nm was measured in order to evaluate the percentage of the intact curcumin (Fig. 9). The percent of intact curcumin retained was calculated relatively to the absorbance at time zero. All samples were prepared a day before 'time zero', and were shaken at 4 °C overnight to reach equilibrium. It is important to note that a preliminary experiment showed that the absorbance spectrum of β-Cg alone in phosphate buffer was not changed during a whole week and there was no visible formation of crystals, aggregation or sedimentation in the solutions. Therefore it was concluded that the decrease in 424 nm absorbance of curcumin - β-Cg solutions resulted only from the degradation of curcumin and not due to dissociation between the β-Cg and curcumin.

As can be seen in Fig. 9, during the 7 days of the accelerated shelf life experiment the percentage of the curcumin

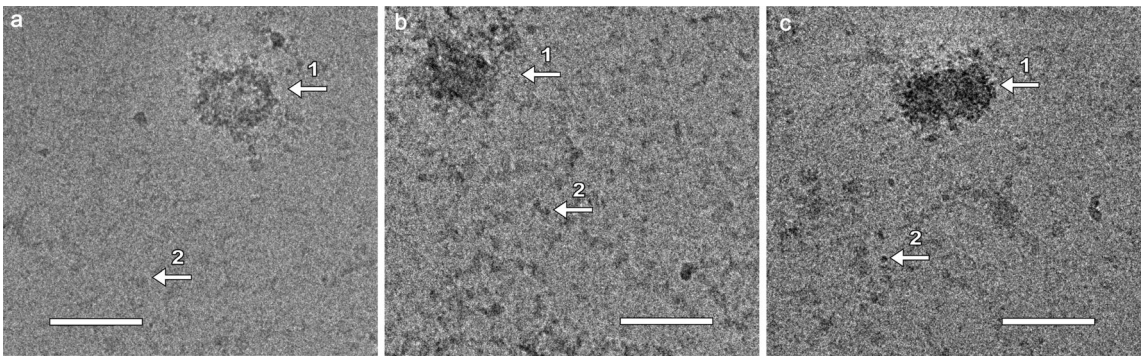


**Fig. 8** Cryo-TEM images of (**a**) 5.26 μM β-Cg in 30 mM phosphate buffer. Arrow 1 points to a large (~ 100 nm) cluster of protein aggregates and arrow 2 shows one of the more numerous, small (~10–20 nm diameter) protein aggregates. Images (**b**) and (**c**): curcumin:β-Cg 3:1 and 6:1 molar ratios. In both images (b and c), arrow 1 most likely shows a large cluster of protein co-assembled with curcumin (seen as darker dots). Likewise, arrows 2 point to small protein nanoparticles, co-assembled with curcumin. Scale bars: 100 nm

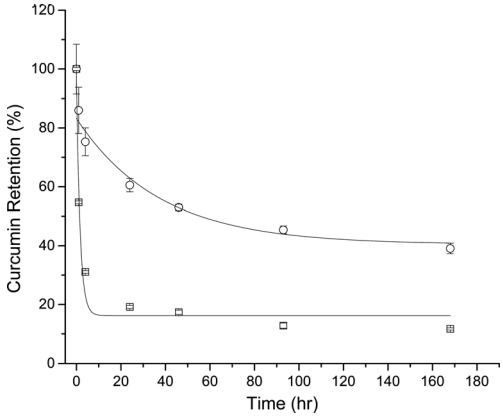


**Fig. 9** Accelerated shelf life test: Percent of remaining curcumin in solutions initially containing 15 μM curcumin with (circles) and without (squares) 5.26 μM (1 mg/ml) β-Cg in 30 mM phosphate buffer. The solutions were exposed to light and oxygen and were continuously shaken at room temperature. The % of curcumin retained was determined by absorbance at 424 nm, and calculated relatively to the absorbance at time zero. Curve-fits represent first-order kinetics approximation

decreased in all solutions. However, pure curcumin dispersion showed the fastest decrease, and within 1 h, almost 50 % of the initial curcumin there was lost. In contrast, in the presence of β-Cg only 10% of the initial curcumin was lost, and after a week more curcumin remained in the presence of β-Cg (40%) compared to in its absence (10%). Therefore, it can be concluded that β-Cg conferred significant protection to the encapsulated curcumin against the combined degrading effects of light and oxygen. This protection may be explained by one or a few of several possible mechanisms [51]: β-CG binding to the surface of curcumin nanoparticles may be shielding them from molecular oxygen, free radicals, transition metal ions, and possibly also from incident light, thus slowing curcumin decay.

To compare between the soy protein protection of curcumin and the protection provided by other technologies we assumed degradation according to first order kinetics, and used OriginLab to fit the data. The curve fits are presented in Fig. 9, and the values for k, the decay constant, and $t_{1/2}$, the half-life, are presented in Table 1. The decay constant obtained for curcumin at pH 6.8 was 0.612 $h^{-1}$ and the half-life was 1.132 h. Tønnesen et al. found similar values for the photochemical degradation of curcumin dissolved in ethanol:phosphate buffer pH 5 (40:60): k=0.588 $h^{-1}$ and $t_{1/2}$=1.18 h [7].

**Table 1** First-order decay parameters for curcumin degradation during accelerated shelf life test

| | K (1/h) | Standard Error | $t_{1/2}$ (hr) | Standard Error |
|---|---|---|---|---|
| Curcumin | 0.612 | 0.144 | 1.1 | 0.3 |
| Curcumin protected by β-Cg | 0.027 | 0.006 | 25.7 | 5.5 |

In the presence of β-Cg, curcumin decayed with an approximately tenfold lower rate constant, k=0.027 $h^{-1}$, and tenfold higher $t_{1/2}$: 25.746 h. As was concluded above, it can be seen that in the presence of β-Cg, curcumin degradation rate is about one order of magnitude lower!

Tønnesen et al. investigated the photochemical degradation rate of curcumin complexed with cyclodextrin molecules in aqueous medium [7]. They found first order decay constants between 0.9 and 2.04 $h^{-1}$ and $t_{1/2}$ between 0.34 and 0.77 h for six different derivatives of cyclodextrin at pH 5. Hence, β-Cg seems to provide better protection for curcumin compared to cyclodextrin, which is reasonable, as in cyclodextrin the curcumin is molecularly entrapped, and is still quite exposed to the solvent, while in β-Cg, curcumin seems to be entrapped as small nanoaggregates (possibly crystalline) and the protein is much larger and hence provides much better shielding from the solvent compared to cyclodextrin. Moreover, the protein may absorb some of the UV radiation which may deteriorate curcumin, while cyclodextrin can hardly absorb such radiation or shield the entrapped molecule from light.

## Conclusions

The main objective of the current project was to study the possibility of using the soybean protein, β-Cg, as protective nanovehicle for delivery of curcumin in clear beverage solutions. Particularly, to quantify the binding of curcumin by β-Cg at neutral pH values, typical for a major beverage category, mineral water (6.7–7.3) and for water enriched with vitamins and nutraceuticals. Moreover, we aimed to characterize the binding of curcumin to β-Cg and the loading capacity, to quantify the transparency and the particle size distribution at varying curcumin and β-Cg concentrations, and to evaluate colloidal stability and degradation of the curcumin with and without complexation with the protein.

We found that the β-Cg – curcumin complexes system was characterized by significantly smaller and colloidally-stable nanoparticles compared to the dispersion of curcumin alone, which formed unstable crystalline microparticles. By varying curcumin and β-Cg concentrations, stable yellowish transparent solutions were obtained.

Two different data analysis methods of the spectrophotometry results yielded mutually supportive values for the binding constant of curcumin and β-Cg (average result $1.27 \cdot 10^6$ $M^{-1}$) and a binding ratio of ~1:1 was obtained. This indicates high affinity binding between β-Cg and curcumin. However, DLS and microscopy data suggest that, in fact, nanoaggregates (or nanocrystals) of curcumin are entrapped within the protein nanoparticles, and the protein maximal molar loading capacity is about 15:1 (~3 g curcumin per 100 g protein).

The nanoparticles of β-Cg curcumin showed bimodal size distributions with a major sub-population ranging 20–70 nm and a minor sub-population ranging 70–200 nm. The average size in the range of 3:1–15:1 was 46 nm.

When evaluating the protection conferred by β-Cg to curcumin during an accelerated shelf life stress test, significant protection was observed against exposure to light and oxygen induced degradation. Assuming first order kinetics, a decay constant of 0.612 $h^{-1}$ and a half-life of 1.1 h were observed for curcumin, while for curcumin in the presence of β-Cg a decay constant of 0.027 $h^{-1}$ and $t_{1/2}$ of 25.7 h were observed, representing a ten-fold slower degradation rate. Further study would be needed for exploring the mechanisms of protection against light-induced- and against oxygen-induced degradations. Also, the performance of the nano-complexes through simulated gastric digestion should be studied, as it is likely that the entrapment in β-Cg would improve the bioavailability compared to that of pure curcumin aggregates, thanks to the larger surface-to-volume ratio, and the suppression of crystallization of the bioactive, which is now under study in our lab.

We conclude that β-Cg is a good potential nanocarrier for hydrophobic nutraceuticals, curcumin in particular, in clear neutral-pH beverages, and most probably in other food and beverage products.

**Acknowledgments** The study was supported by the Nofar program, Israeli Ministry of Economy, and by Solbar Ltd. (Ashdod, Israel, CHS Inc. Minnesota, USA). The authors thank Maya Bar-Zeev for her help with light microscopy, and Dr. Ellina Kesselman, for her help with the cryoTEM.

## References

1. R.A. Sharma, A.J. Gescher, W.P. Steward, Eur. J. Cancer **41**(13), 1955–1968 (2005)
2. A. Barik, K.I. Priyadarsini, H. Mohan, Photochem. Photobiol. **77**(6), 597–603 (2003)
3. K.I. Priyadarsini, J. Photochem. Photobiol. C: Photochem. Rev. **10**(2), 81–95 (2009)
4. R.K. Maheshwari, A.K. Singh, J. Gaddipati, R.C. Srimal, Life Sci. **78**(18), 2081–2087 (2006)
5. B.B. Aggarwal, A. Kumar, A.C. Bharti, Anticancer Res. **23**(1A), 363–398 (2003)
6. E. Kunchandy, M.N.A. Rao, Int. J. Pharm. **58**(3), 237–240 (1990)
7. H.H. Tønnesen, M. Másson, T. Loftsson, Int. J. Pharm. **244**(1–2), 127–135 (2002)
8. T. Masuda, K. Hidaka, A. Shinohara, T. Maekawa, Y. Takeda, H. Yamaguchi, J. Agric, Food Chem. **47**(1), 71–77 (1999)
9. A.C. Reddy, B.R. Lokesh, Mol. Cell. Biochem. **111**(1–2), 117–124 (1992)
10. Y.-J. Wang, M.-H. Pan, A.-L. Cheng, L.-I. Lin, Y.-S. Ho, C.-Y. Hsieh, J.-K. Lin, J. Pharm, Biomed. Anal. **15**(12), 1867–1876 (1997)
11. H.B. Sowbhagya, S. Smitha, S.R. Sampathu, N. Krishnamurthy, S. Bhattacharya, J. Food Eng. **67**(3), 367–371 (2005)
12. A.H. Sneharani, J.V. Karakkat, S.A. Singh, A.G.A. Rao, J. Agric, Food Chem. **58**(20), 11130–11139 (2010)
13. Y.D. Livney, Curr. Opin. Colloid Interface Sci. **15**(1–2), 73–83 (2010)
14. M. Haham, S. Ish-Shalom, M. Nodelman, I. Duek, E. Segal, M. Kustanovich, Y.D. Livney, Food Funct. **3**(7), 737–744 (2012)
15. E. Semo, E. Kesselman, D. Danino, Y.D. Livney, Food Hydrocoll. **21**(5–6), 936–942 (2007)
16. P. Zimet, D. Rosenberg, Y.D. Livney, Food Hydrocoll. **25**(5), 1270–1276 (2011)
17. G. Markman, Y.D. Livney, Food Funct. **3**, 262–270 (2012)
18. A. Shpigelman, G. Israeli, Y.D. Livney, Food Hydrocoll **24**(8), 735–743 (2010)
19. A. Shpigelman, Y. Cohen, Y.D. Livney, Food Hydrocoll. **29**(1), 57–67 (2012)
20. N. Ron, P. Zimet, J. Bargarum, Y.D. Livney, Int. Dairy J. **20**(10), 686–693 (2010)
21. P. Zimet, Y.D. Livney, Food Hydrocoll. **23**(4), 1120–1126 (2009)
22. R.Y. Yada, *Proteins in food processing.* (Woodhead Publishing, 2004).
23. K. Nishinari, Y. Fang, S. Guo, G.O. Phillips, Food Hydrocoll. **39**, 301–318 (2014)
24. J.E. Kinsella, J. Am, Oil Chem. Soc. **56**(3), 242–258 (1979)
25. S. Utsumi, Y. Matsumura and T. Mori, in *Food Proteins and Their Applications*, edited by S. Damodaran and A. Paraf (Dekker, New York, 1997), pp. 257–291.
26. V.H. Thanh, K. Shibasaki, J. Agric, Food Chem. **26**(3), 692–695 (1978)
27. N. Maruyama, R. Sato, Y. Wada, Y. Matsumura, H. Goto, E. Okuda, S. Nakagawa, S. Utsumi, J. Agric, Food Chem. **47**(12), 5278–5284 (1999)
28. N. Maruyama, M. Adachi, K. Takahashi, K. Yagasaki, M. Kohno, Y. Takenaka, E. Okuda, S. Nakagawa, B. Mikami, S. Utsumi, Eur. J. Biochem. **268**(12), 3595–3604 (2001)
29. T. Vu Huu, S. Kazuo, Biochimic. Biophys. Acta (BBA) - Protein Struct. **490**(2), 370–384 (1977)
30. D.E. Roopchand, C.G. Krueger, K. Moskal, B. Fridlender, M.A. Lila, I. Raskin, Food Chem. **141**(4), 3664–3669 (2013)
31. M.H. Grace, I. Guzman, D.E. Roopchand, K. Moskal, D.M. Cheng, N. Pogrebnyak, I. Raskin, A. Howell, M.A. Lila, J. Agric, Food Chem. **61**(28), 6856–6864 (2013)
32. Z.L. Wan, J.M. Wang, L.Y. Wang, Y. Yuan, X.Q. Yang, Food Chem. **161**, 324–331 (2014)
33. A. Tapal, P.K. Tiku, Food Chem. **130**(4), 960–965 (2012)
34. Y. Levinson, G. Israeli-Lev, Y. Livney, Food Biophys. **9**(4), 332–340 (2014)
35. T. Vu Huu, K. Shibasaki, J. Agric, Food Chem. **27**(4), 805–809 (1979)
36. D.M. Shuttuck-Eidens, R.N. Beachy, Plant Physiol. **78**(4), 895–898 (1985)
37. E. Reverchon, J. Supercrit. Fluids **15**(1), 1–21 (1999)
38. D.A. Dougherty, J. Org. Chem. **73**(10), 3667–3673 (2008)
39. H.E. Rosenthal, Anal. Biochem. **20**(3), 525–532 (1967)
40. C.A. Schalley, *Analytical Methods in Supramolecular Chemistry.* (Wiley, 2012).
41. Anon, Parafilm$^{(R)}$ M BRAND GMBH Germany, (2009), Accessed: 27.1.14 http://www.brand.de/fileadmin/user/pdf/Leaflets/PARAFILM_EN.pdf
42. R.K. Singh, D. Rai, D. Yadav, A. Bhargava, J. Balzarini, E. De Clercq, Eur. J. Med. Chem. **45**(3), 1078–1086 (2010)
43. E.V. Anslyn and D.A. Dougherty, *Modern Physical Organic Chemistry.* (University Science, 2006).
44. Z. Teng, Y.C. Luo, Q. Wang, J. Agric, Food Chem. **60**(10), 2712–2720 (2012)
45. A. Dongre, P. Bhisey and U. Khopkar, *Polarized light microscopy.* (2007).

46. A. Shpigelman, Y. Shoham, G. Israeli-Lev, Y.D. Livney, Food Hydrocoll. **40**, 214–224 (2014)
47. A. Shapira, I. Davidson, N. Avni, Y.G. Assaraf, Y.D. Livney, Eur. J. Pharm. Biopharm. **80**(2), 298–305 (2012)
48. Z. Jia, P.L. Davies, Trends Biochem. Sci. **27**(2), 101–106 (2002)
49. A.C. Doxey, M.W. Yaish, M. Griffith, B.J. McConkey, Nat. Biotech. **24**(7), 852–855 (2006)
50. M.P. Nori, C.S. Favaro-Trindade, S. Matias de Alencar, M. Thomazini, J.C. de Camargo Balieiro, C.J. Contreras Castillo, LWT Food Sci. Technol. **44**(2), 429–435 (2011)
51. Y.D. Livney, in *Encapsulation technologies and delivery systems for food ingredients and nutraceuticals*, edited by N. Garti and D. J. McClements (Woodhead Publishing Limited, Oxford, Cambridge, Philadelphia, New Delhi, 2012).